Supporting Information

Multifunctional Compartmentalized Capsules with a Hierarchical Organization from the Nano to the Macro Scales

Rui R. Costa[a,b], Emilio Castro[a,b], F. Javier Arias[c,d], J. Carlos Rodríguez-Cabello[c,d] and João F. Mano [a,b,*]

[a]3B's Research Group – Biomaterials, Biodegradables and Biomimetics, University of Minho, Headquarters of the European Institute of Excellence on Tissue Engineering and Regenerative Medicine, AvePark, Zona Industrial da Gandra, S. Cláudio do Barco, 4806-909 Caldas das Taipas – Guimarães, Portugal.

[b]ICVS/3B's, PT Government Associated Laboratory, Braga/Guimarães, Portugal.

[c]G.I.R. Bioforge, University of Valladolid, Edificio I+D, Paseo de Belén, 1, 47011, Valladolid, Spain.

[d]Networking Research Center on Bioengineering, Biomaterials and Nanomedicine (CIBER-BBN), Valladolid, Spain.

*corresponding author: jmano@dep.uminho.pt

INDEX

1. Deacetylation degree of chitosan.

Hydrogen-1 nuclear magnetic resonance (^{1}H-NMR) spectra were recorded using a Varian MR-400 spectrometer to determine the deacetylation degree (DD) of chitosan. Thus, 10 mg of chitosan was dissolved in 1 mL of deuterated water (D_2O) and 20 µL of deuterated hydrochloric acid (DCl) to form a viscous solution. An aliquot of this solution was placed in a 5 mm NMR tube and the spectrum recorded at 60 °C.

The calculation of the deacetylation degree, DD, was described by Hirai et al (Hirai, A.; Odani, H.; Nakajima, A. *Polym. Bull.* **1991**, *26*, 87-94) and is presented in Equation S1:

$$DD(\%) = \left[1 - \left(\frac{\frac{1}{3}I_e}{\frac{1}{6}I_c}\right)\right] \times 100 \qquad \text{(S1)}$$

where I_x is the area of each of the peaks (x) identified in Figure S1. The *DD* of the purified chitosan used was 81.6%.

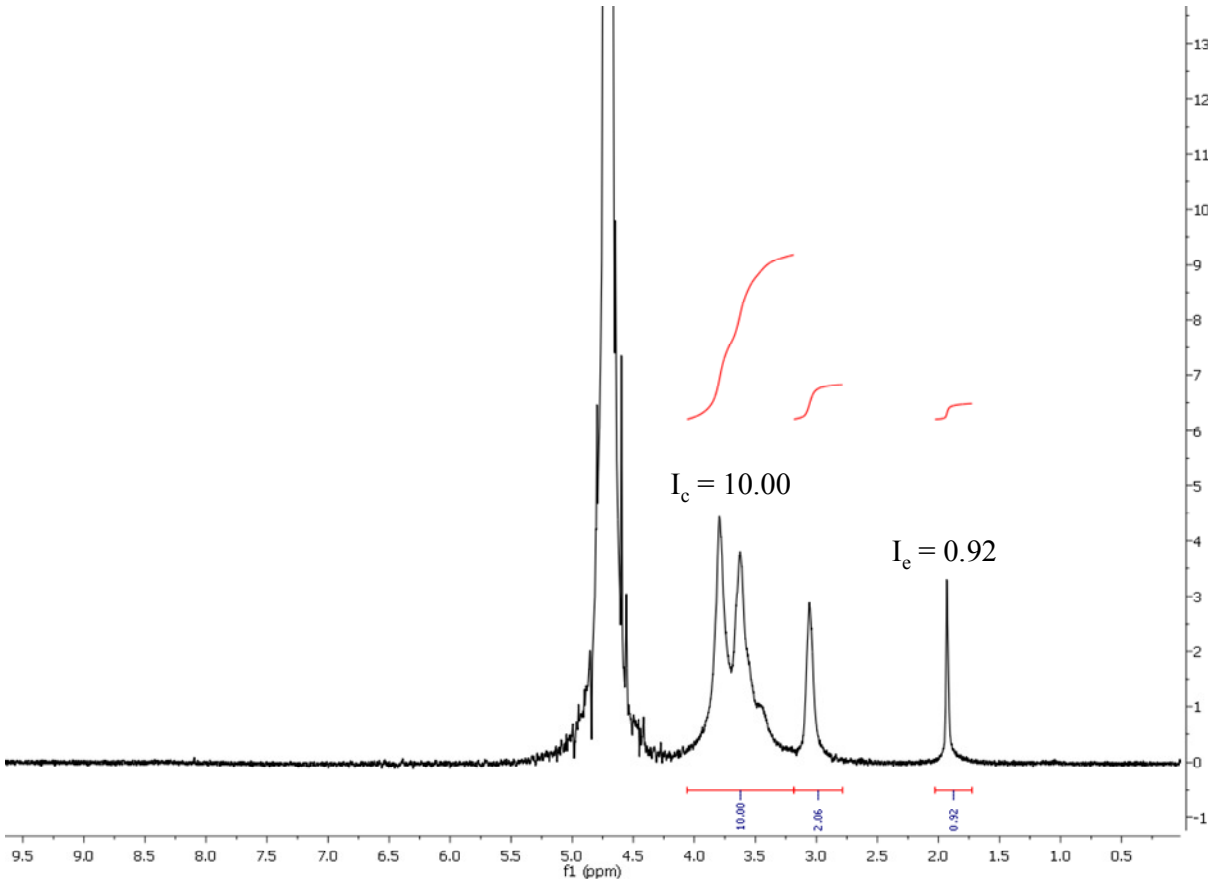

Figure S1. ^{1}H-NMR spectrum of the purified chitosan sample, with 10.00 corresponding to I_c peak and 0.92 to I_e peak.

2. ELR transition temperature

The aggregate sizes of ELR in solution were measured using a Nano-ZS from Malvern (United Kingdom) in the temperature range 25–37 °C after stabilization for 5 minutes. Samples were prepared at 300 μg•mL^{-1} in PBS, pH 7.4. A total of 20 runs were performed for each sample to obtain an average value at stabilized temperature.

In order to evaluate the thermal response of the featured ELR, the size variations of peptide aggregates in aqueous solution were measured as a function of temperature in small increments. It can be seen from Figure S2 that the ELR forms aggregates of 4.4±2.8 nm at 25 °C and 1290±113 nm at 29 °C. This abrupt size variation gives a T_t of 29 °C for the ELR. ELR self-assembly progresses further with increasing temperature.

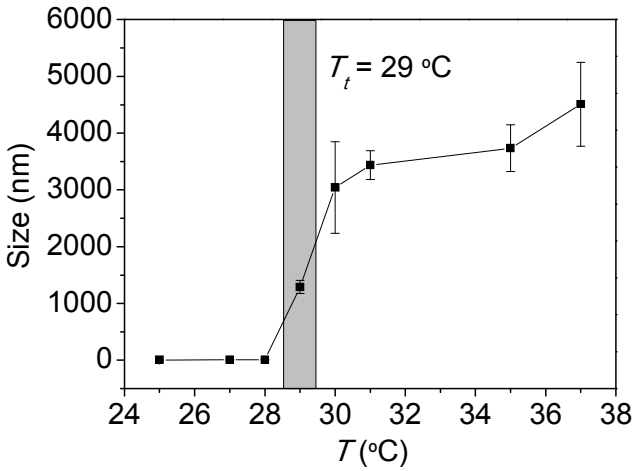

Figure S2. Aggregate size profile for a 300 μg•mL^{-1} ELR solution in PBS over the temperature range, *T*, of 25–37 °C, with two standard deviations represented.

3. Rhodamine encapsulation losses

The encapsulation efficiency of Rhod in either the inner or the external compartments was determined by fluorescence measurements of the retrieved supernatants during their construction using a Synergie HT microplate ELISA reader (BioTek, USA). Thus, 150 μL of sample was pipetted into white, opaque 96-well plates in triplicate. Ultrapure water was used as blank. The excitation (λ_{exc}) and emission (λ_{em}) wavelengths used for Rhod mass calculations were 530 and 590 nm, respectively. All supernatants collected during entrapment, construction and chelation stages were measured and quantified. The percentage Rhod loss was plotted for both each stage and cumulatively.

All the supernatants collected during the construction of Rhod-loaded compartments (either internal or external ones) were used to calculate the losses occurred prior to the commencement of the actual

release studies. The graphic in Figure S3 shows the stage and cumulative Rhod losses with respect to the initial encapsulated mass.

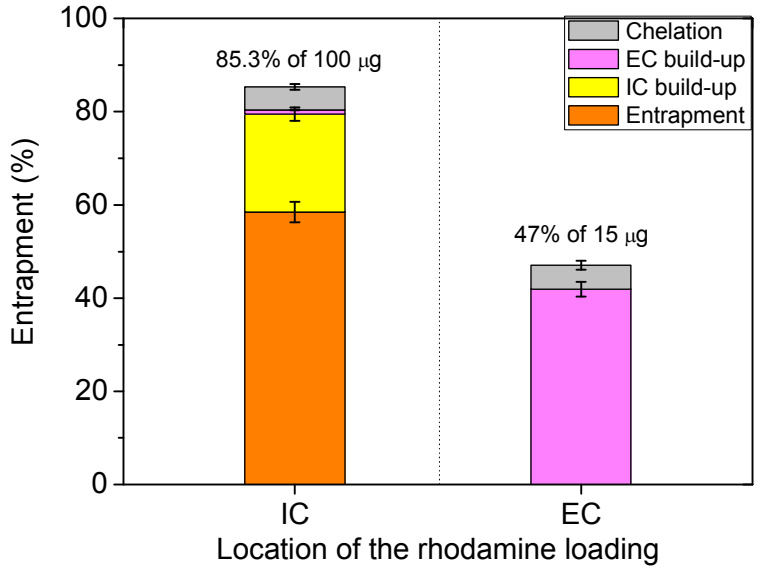

Figure S3. Rhodamine losses during the construction of Rhod-loaded microcapsules (ICs) within macrocapsules (ECs) and empty microcapsules within Rhod-loaded macrocapsules, with two standard deviations represented.

When Rhod was loaded within the inner compartments, the construction process consisted of four stages: (i) entrapment within the CaCO3 particles (orange in the graphic), (ii) build-up of the $(CHI/ELR)_3$ multilayer (yellow), (iii) build-up of the external $(CHI/ALG)_3$ multilayer (purple), and (iv) simultaneous $CaCO_3$ chelation and alginate bead liquefaction (grey). When Rhod was loaded within the external compartments, losses are only present in stages (iii) and (iv), when Rhod is introduced into the system. The sacrificial template was maintained until the end of stage (iii) to prevent early diffusion during the construction. Thus, Rhod could be protected and physically retained within the sacrificial template until the final stage of chelation.

As mentioned previously, the quantity of Rhod loaded initially differed depending on whether it was encapsulated within the internal or the external compartments. As a result, we first quantified the Rhod losses during the construction of ECs containing Rhod-loaded ICs and found that 85% of Rhod had been lost at the end of the construction, thus meaning that only 15 μg of the initial 100 μg were effectively encapsulated at time-point "0". In an attempt to encapsulate roughly the same mass of fluorophore in the ECs, we loaded them with the equivalent quantity of 15 μg of Rhod during the ionic gelation step of 1 mL of alginate. Note that this value disregards the subsequent loss of 47% that was further quantified

following liquefaction of the bead. Furthermore, empty $CaCO_3$-coated particles were loaded at the same time to keep the same subcompartmental structure.

4. Magnetic responsiveness assay

Figure 6c of the main manuscript and Video S2 depict the magnetic responsiveness of the MNP-loaded ICs within ECs. As expected, a group of eight compartmental units were attracted by a magnet placed 3 cm away from their starting point. The normalized distance traveled by each capsule is plotted as a function of time in Figure S4. As soon as the magnetic compartmental units were exposed to the external magnetic field, they became attracted to it. Subsequently they were exposed to an increasingly stronger magnetic field value and the attraction increased. Movement stopped abruptly once they reached the position at which the maximum magnetic field value was available to them.

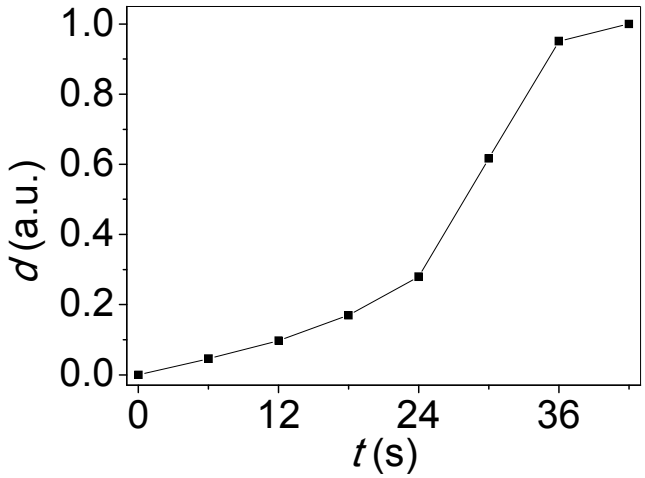

Figure S4. Normalized mean distance, *d* in arbitrary units, traveled by MNP-loaded ICs within ECs as a function of time, *t*, from their starting point to the point of the highest magnetic field value available.